Journal of ELECTRONIC MATERIALS, Vol. 48, No. 11, 2019
https://doi.org/10.1007/s11664-019-07519-6

Effect of Functional Groups on the Thermoelectric Performance of Carbon Nanotubes

XIAOQI LAN,[1,2] CONGCONG LIU,[1] TONGZHOU WANG,[1,4] JIAN HOU,[2] JINGKUN XU,[1] RONGRI TAN,[1,5] GUANGMING NIE,[3] and FENGXING JIANG [1,6]

1.—Department of Physics, Jiangxi Science and Technology Normal University, Nanchang 330013, People's Republic of China. 2.—State Key Laboratory for Marine Corrosion and Protection, Luoyang Ship Material Research Institute, Qingdao 266101, China. 3.—College of Chemistry and Molecular Engineering, Qingdao University of Science & Technology, Qingdao 266042, People's Republic of China. 4.—e-mail: wangtz08@163.com. 5.—e-mail: rrtan@163.com. 6.—e-mail: f.x.jiang@live.cn

Single-wall carbon nanotubes (SWCNTs) have received much attention in the past decade due to their excellent electric and mechanical properties. The quantum confinement effect of charge carriers in an individual carbon nanotube (CNT), together with the flexible topology and high tensile strength, make it a potential candidate thermoelectric (TE) material. However, the low Seebeck coefficient and high thermal conductivity of SWCNTs limits further development for a good TE material with high performance. Although many efforts have been focused on the improvement of TE performance for SWCNTs by doping and composites, few works have been devoted to investigation of functional groups in SWCNTs. In this work, we investigated the TE performance of SWCNT films in detail with different functional groups (hydroxyl, carboxyl, and amino). It is found that the Seebeck coefficient of SWCNTs with different functional groups have an obvious improvement with the decrease in electrical conductivity. An optimal power factor of 47.8 μW m^{-1} K^{-2} was obtained for SWCNTs with a hydroxyl group comparable to pure SWCNTs. Significantly, the introduction of functional groups results in a marked reduction in thermal conductivity and an enhanced TE figure of merit (ZT). This work provides an alternative strategy to optimize the TE performance of SWCNTs.

Key words: Thermoelectric performance, functionalized carbon nanotube, Seebeck coefficient, power factor

INTRODUCTION

Recently, thermoelectric (TE) materials have received extensive attention in both industry and academy due to the ability to convert waste heat to electricity without moving parts and bulk fluids.[1–3] The energy conversion efficiency of TE materials can be evaluated by a dimensionless figure of merit (ZT), expressed by $ZT = \sigma S^2 T/\kappa$, wherein σ is electrical conductivity, S is the Seebeck coefficient, T is the absolute temperature, and κ is the thermal conductivity.[4–6] In order to achieve a high TE performance, a number of different inorganic and organic materials have been explored for their potential in TE energy harvesting devices.[6–8]

Among these materials, carbon-based TE materials have received much attention in the past decade due to the high electrical conductivity, large surface area, abundant source, and easier processability. Single-wall carbon nanotubes (SWCNTs) are a representative of carbon materials with an extremely stable one-dimensional (1D) nanostructure

(Received April 10, 2019; accepted August 1, 2019; published online August 9, 2019)

and high electrical conductivity as well as good mechanical performance.[9–11] SWCNTs have been regarded as a potential candidate due to their low resistivity and large Seebeck coefficient. Importantly, owing to the unique 1D nanoscale systems, the inherent quantum confinement effect and large surface-to-volume ratio for SWCNTs can effectively confine charge carriers and thermal transports and yield boundary inelastic scattering benefit for improving TE performance.[12–15] Moreover, SWCNTs can be easily doped due to practical defects, including vacancy and conformation, even by simply soaking and applying surface-chemisorbed molecules to tune its thermal and TE properties.[16] Nonoguchi and co-workers have achieved a large improvement of TE performance for carbon nanotubes (CNTs) using a variety of weak electron donors.[17] Carroll et al. reported a TE fabric with high power output based on CNTs and polyvinylidene fluoride.[10] Xie et al. fabricated flexible CNT films with an ultrahigh power factor and long-term stability by doping with polyethyleneimine.[11] Pedgett and Brenner found the functionalization by chemical attachment of phenyl rings sharply reduces the thermal conductivity of CNTs.[18] Much literature has reported that the surface functionalization of carbon-based materials, such as CNTs and graphene, can further change the chemical and physical properties, allowing the materials to be used in sensors and catalysts.[19–23] Nevertheless, there are few experimental efforts that have been devoted to the investigation of the TE performance of SWCNTs with different functional groups.

In this work, we investigated the functionalization of hydroxyl, carboxyl, and amino groups and their effects on the TE performance of SWCNTs. It can be found that functional groups result in a significant improvement in the Seebeck coefficient of SWCNTs and a marked reduction in their electrical conductivity. Moreover, the different functional groups have different effects on the TE power factor of SWCNTs. It is certain that the introduction of functional groups significantly reduces the thermal conductivity of SWCNTs, ultimately leading to an increase in ZT values, which provides a new strategy for optimizing the TE property of SWCNTs.

EXPERIMENTAL SECTION

Materials

As mentioned, the CNTs used in this work are SWCNTs. The functionalized CNTs are also SWCNTs including hydroxyl (–OH), carboxyl (–COOH), and amino ($–NH_2$) groups. The surfactant used for dispersion of SWCNTs is an alcohol polymer dispersant designed as XFZ21. The SWCNTs and surfactant were purchased from Nanjing XFNANO Materials Tech Co. Ltd. The types of SWCNTs are XFS05 for the pure SWCNTs, XFS06 for SWCNT-OH, XFS15 for SWCNT-COOH, and XFS15 for SWCNT-NH_2.

Fabrication of SWCNT Films

SWCNT powder (15 mg) was dispersed into 15 ml of deionized water with 5 mg of polymer surfactant. Then, the resultant mixtures were sonicated for 1 h. The SWCNT films were fabricated through direct-vacuum filtration with a porous polyvinylidene difluoride (PVDF) membrane (pore size: 0.45 mm) and dried at 60°C in a vacuum oven for 30 min. The SWCNT-OH, SWCNT-COOH, and SWCNT-NH_2 films were also prepared by the same method. The as-fabricated SWCNT films were rinsed repeatedly with deionized water to remove the excess surfactant. The thickness of all samples was measured between 1.0 μm and 1.5 μm by a thickness gauge. Scheme 1 shows the preparation of SWCNT films via a vacuum filtration method.

Measurement and Instrumentation

Scanning electron microscopy (SEM) images were obtained using a JSM-7500F instrument (JEOL, Japan). Raman spectra were recorded by HR-800 (Horiba Jobin–Yvon, France) at an excitation length of 633 nm. The chemical composition and structure of SWCNTs were analyzed by x-ray photoelectron spectroscopy (XPS) with an Escalab 250 Xi instrument from Thermo Fisher Scientific. The in-plane thermal conductivity of SWCNTs was determined by 3ω method using LINSEIS TFA. Keithley 2700 equipment was employed to detect the electrical conductivity films via a standard four-point-probe technique. During this measure, a rectangle-shaped film with the PVDF substrate (9 mm $\times$ 2 mm) was glued to the two cross-linked glass substrates using silver paste. The whole system was controlled by a computer equipped with LabVIEW software. A temperature difference ΔT across the sample created by thermal resistance (1000 Ω) served as the heat source connecting a Keithley 2401 and was detected by a pair of platinum thermometers (Pt100). The Keithley 2700 was used to measure the TE voltage (ΔV) induced by the temperature difference. The Seebeck coefficient is calculated by $S = -\Delta V/\Delta T$, where ΔV and ΔT are the voltage drop in response to the material and the temperature gradient along the voltage, respectively. The ΔT was controlled to be 5 K by LabVIEW software.

RESULTS AND DISCUSSION

Figure 1 shows the SEM images of as-fabricated SWCNT, SWCNT-OH, SWCNT-COOH, and SWCNT-NH_2 . There is no obvious difference among SWCNT films before and after functionalization. Macroscopically, one can observe that the as-fabricated SWCNTs belong to the low-density bulk mat films obtained by direct filtering. It was apparent that SWCNTs randomly intertwined together, and their bundles show the spaghetti-like morphology to allow a good conductive network, which is a benefit to the transport of charge carriers and the

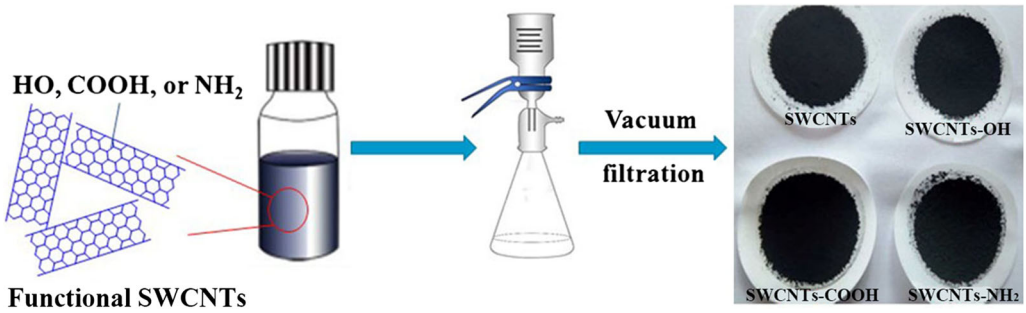

Scheme 1. Schematic illustration of different SWCNT films by dilution-filtration.

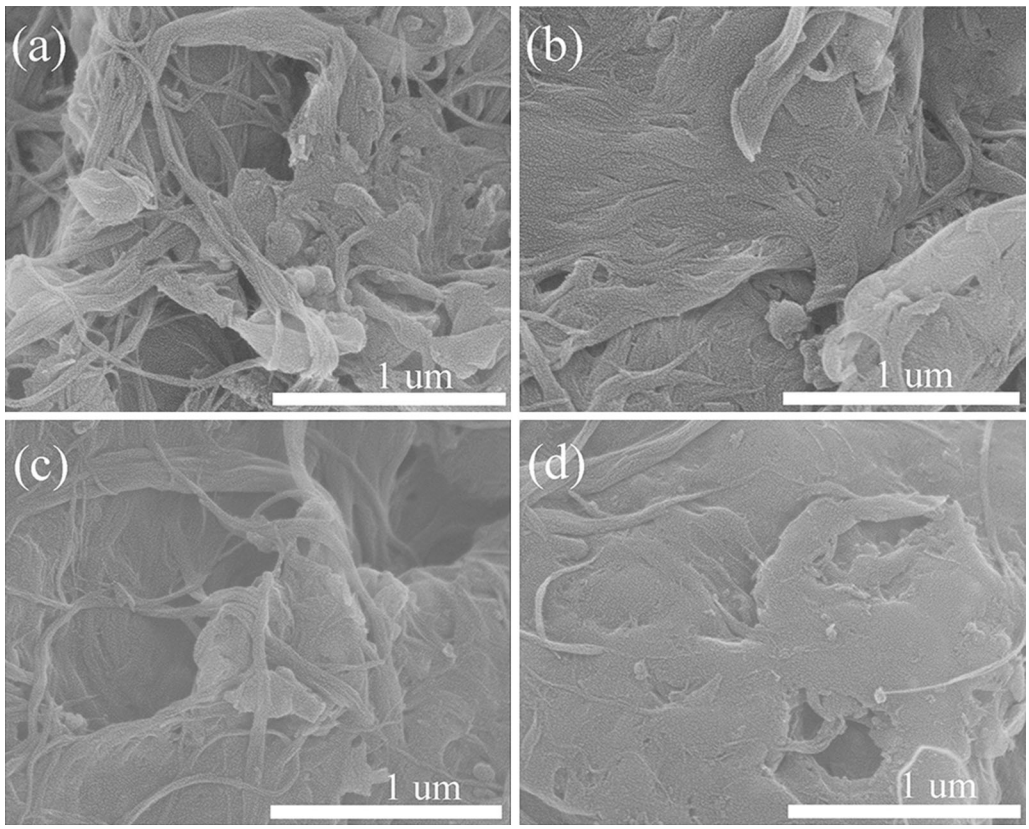

Fig. 1. SEM images of SWCNT (a), SWCNT-OH (b), SWCNT-COOH (c), and SWCNT-NH_2 (d) films.

improvement of electrical conductivity.[12] It is difficult for the individual SWCNTs to be distinguished owing to the residual polymer surfactant, although the as-fabricated films were rinsed repeatedly with deionized water.

As shown in Fig. 2, Raman spectra provide an insight into the structural differences for pristine and functional SWCNTs. One can see that the Raman spectra of different SWCNTs revealed the characteristic peaks including D, G, and 2D bands.[19] As we know, the D mode is sp^3-hybridized carbons and assigned to the edges and structural defects of the lattice in the SWCNT, while the G band at 1590 cm^{-1} is caused by the E_{2g} vibration mode of sp^2 carbon atoms.[24] It is noted that almost no D band ($\sim$ 1350 cm^{-1}) can be observed for pure SWCNTs, suggesting a better semi-metallic structure. In contrast, the functionalization results in an increased peak intensity indicating the introduction of defects in the SWCNTs. Moreover, the intensity ratio of D/G shows obvious change, suggesting various degrees of functionalization for pure SWCNT (0.008), SWCNT-OH (0.09), SWCNT-COOH (0.11), and SWCNT-NH_2 (0.16), and the continuous delocalization of electrons throughout the nanotubes had been highly disrupted.[19] This

probably leads to a large change in TE performance due to the introduction of functional groups in SWCNTs.

To further confirm the functionalization, Fig. 3 exhibits the C 1s, N 1s (inset), and O 1s (inset) XPS spectra of different SWCNTs. As shown in Fig. 3, the C 1s spectrum of SWCNTs in the XPS spectra are divided into several bands consisting of C–C (284.7 eV), C–O (285.2 eV), and C=O (286.8 eV) functional groups, further demonstrating the introduction of corresponding functional groups in SWCNTs. These results in the inset of Fig. 3 also indicate the functional degree of –OH and –COOH in SWCNTs. It is worth mentioning that pure SWCNTs in Fig. 3a also have a certain degree of defects, but they are much smaller compared to SWCNT-OH (Fig. 3b) and SWCNT-COOH (Fig. 3c). The presence of the N 1s spectrum (inset of Fig. 3d) indicates the successful functionalization of the –NH_2 group. These results are also in close agreement with the Raman spectra and suggest that the sp^3 defects have created and inevitably led to the change in electronic structure of the SWCNTs.

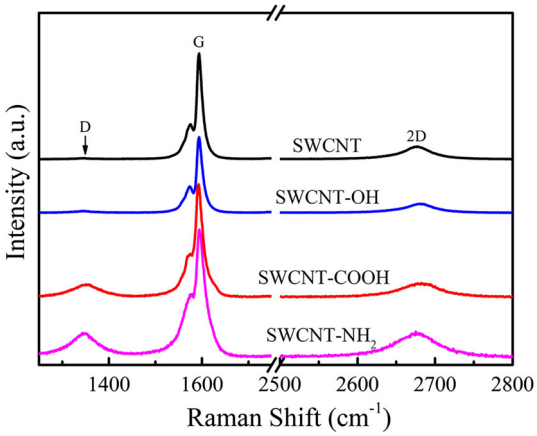

Fig. 2. Raman spectra of SWCNT (a), SWCNT-OH (b), SWCNT-COOH (c), and SWCNT-NH_2 (d).

Theoretically, the pure SWCNTs are allowed to have a large Seebeck coefficient and high electrical conductivity after doping, both being attributed to the position of the Fermi energy and their diameter.[25–27] The TE performance of SWCNTs can be tuned and allowed for band gap engineering by the introduction of functional groups attached to the SWCNT sidewall.[28] As shown in Fig. 4a, it is clear

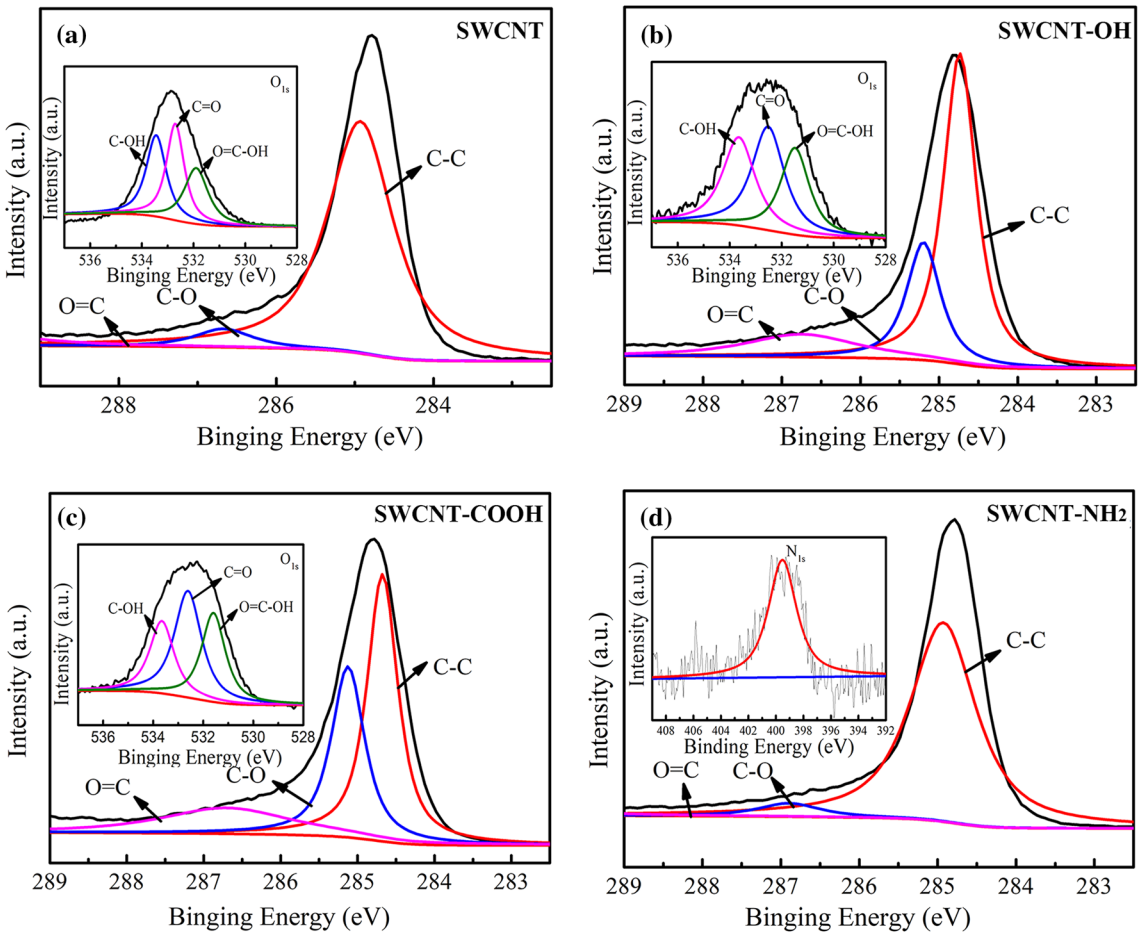

Fig. 3. C 1s XPS spectra of SWCNT (a), SWCNT-OH (b), SWCNT-COOH (c), and SWCNT-NH_2 (d) with an inset of the O 1s and N 1s spectra.

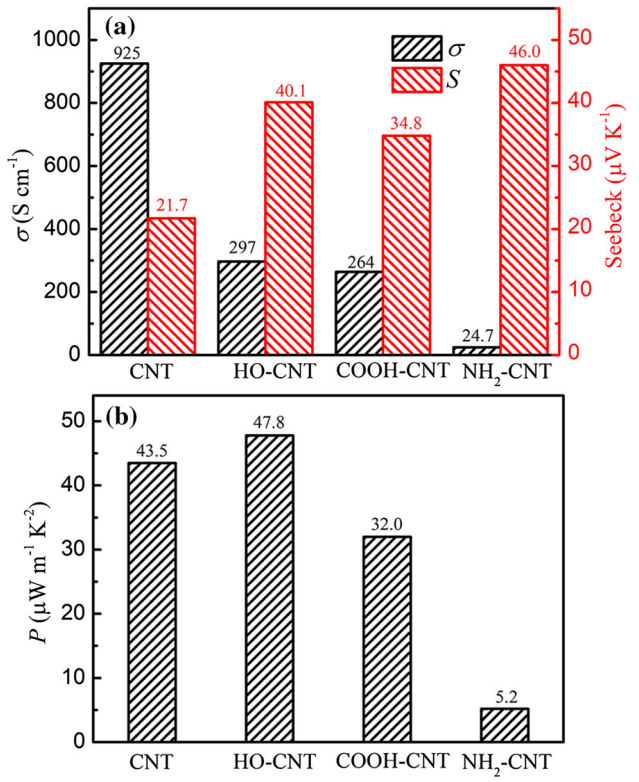

Fig. 4. Electrical conductivity, Seebeck coefficient (a), and power factor (b) of SWCNT, SWCNT-OH, SWCNT-COOH, and SWCNT-NH_2 films.

that the electrical conductivity of functional SWCNT films are much lower than pure SWCNT (925 S cm^{-1}), which was close to the reported values.[13] The electrical conductivity of SWCNT-OH, SWCNT-COOH, and SWCNT-NH_2 films are 297 S cm^{-1}, 264 S cm^{-1}, and 24.7 S cm^{-1}, respectively. After functionalization, although the structures of either the valence or conduction band of SWCNTs have less tremendous change, all the functional groups can induce the carbon hybridization from sp^2 to sp^3, which has been demonstrated by Raman spectra in Fig. 2. This phenomenon induces the half-occupied impurity state around the Fermi level, and these impurity states could act as strong scattering centers of conducting carriers near the Fermi energy level, thus significantly affecting the carrier transport of nanotubes.[29] In other words, the introduction of –OH, –COOH, and –NH_2 will inevitably lead to the increase in resistance due to the defects. The electrical conductivity of SWCNT-NH_2 is much lower than the others. This is ascribed to the many more defects in SWCNT-NH_2, which is agreement with the results of Raman spectra. Milowska and Majewski found that a smaller change in structure of CNTs can be caused by attaching –OH and –COOH compared to other functional groups by theoretical predictions.[28] In theory, a greatly reduced electrical conductivity is not a good phenomenon for an ideal TE material. However, TE performance does not depend solely on electrical conductivity.

The enhancement of Seebeck coefficient is another more important aspect of improving TE performance due to its square. One can see that the Seebeck coefficient of SWCNTs with different functional groups is indicative of the typical *p*-type semiconductors. The pure SWCNT has a low Seebeck coefficient of 21.7 $\mu V\ K^{-1}$ at room temperature with the high electrical conductivity, indicating the very narrow metallic band of pristine SWCNTs.[30] On the other hand, the Seebeck coefficient of SWCNT-OH, SWCNT-COOH, and SWCNT-NH_2 films are significantly enhanced to 40.1 $\mu V\ K^{-1}$, 34.8 $\mu V\ K^{-1}$, and 46.2 $\mu V\ K^{-1}$, respectively, values which are similar to the previous reports.[14,17] Such a significant increase in Seebeck coefficient can be attributed to all the functional groups being able to form covalent bonds with the CNT and induce the local conversion of sp^2- to sp^3-hybridized bonding. These defects caused by sp^3-hybridized bonding have a significant effect on the charge carrier scattering, therefore resulting in a decreased charge carrier concentration and an increased Seebeck coefficient. As we know, the functionalization by attaching covalent groups can lead to the conversion from metallic or semi-metallic to semiconductor for SWCNTs. Moreover, this allows energy mismatch between sp^2-hybridized bonding and sp^3-hybridized bonding benefit the formation of a potential energy barrier. The low-energy carriers may be impeded by the high-energy potential barrier, and the high-energy carriers were allowed to pass through, resulting in an enhanced Seebeck coefficient. The relatively high Seebeck coefficient of SWCNT-NH_2 films was due to the more structural defects, consistent with the Raman results. Overall, the functionalized SWCNTs have a significantly increased Seebeck coefficient compared with pure SWCNTs, the maximum value of which can be observed for SWCNT-NH_2 films (46.2 $\mu V\ K^{-1}$) which is about two times that of the pure SWCNTs without functionalization. In addition, there are different effects on the electrical conductivity and Seebeck coefficient among the three functional groups, which indicates that the Seebeck coefficient is mainly affected by the defects resulting in charge carrier scattering.

On the basis of the electrical conductivity and Seebeck coefficient, the power factor of different SWCNTs was calculated, as shown in Fig. 4b. The power factors of SWCNT, SWCNT-OH, SWCNT-COOH, and SWCNT-NH_2 films are 43.5 $\mu W\ m^{-1}\ K^{-2}$, 47.8 $\mu W\ m^{-1}\ K^{-2}$, 32.0 $\mu W\ m^{-1}\ K^{-2}$, 5.2 $\mu W\ m^{-1}\ K^{-2}$, respectively. Thus, the SWCNT-OH shows the higher TE power factor compared to other functionalized SWCNTs. These values are much lower than the CNTs treated by nitric acid and O_2-doped and similar to the CNTs treated by sulfuric acid and water vapor (Table I). Although the power factor of SWCNTs has not been

Table I. TE performance of different CNT films at room temperature

Dopant	σ (S cm^{-1})	S (μV K^{-1})	σS^2 (μW m^{-1} K^{-2})	κ (W m^{-1} K^{-1})	$ZT \times 10^{-2}$	Refs.
Nitric acid	670	35	85	–	–	31
O_2-doped	512	38	73.9	–	–	32
Sulfuric acid	1100	15.5	26.4	–	–	33
Water vapor	40	50	11.2	–	–	34
SWCNTs	925	21.7	43.5	0.68	1.9	This work
SWCNT-OH	297	40.1	47.8	0.37	3.8	
SWCNT-COOH	264	34.8	32.0	0.41	2.3	
SWCNT-NH_2	24.7	46	5.2	0.24	0.68	

significantly improved after functionalization, the introduction of some functional groups has led to a significant decrease. This does not mean that functionalization is not an optional method for regulating TE performance.

As we know, the thermal conductivity in low-dimensional materials is an important parameter related to the TE property. The thermal conductivity of different SWCNTs varies greatly from 10^3 W m^{-1} K^{-1} to 10^{-1} W m^{-1} K^{-1} depending on chirality, diameter, synthesis method, and so on.[15] A decreased thermal conductivity is desired for SWCNTs as a TE material which can be achieved by introduction of defects or composite.[16,35] Pedgett and Brenner have demonstrated that the function of CNTs with phenyl rings by chemical attachment sharply reduces their thermal conductivity.[18] The in-plane thermal conductivity of SWCNT films was measured and recorded in Table I. One can find that the as-fabricated pure SWCNT film shows a low value of 0.68 W m^{-1} K^{-1} similar to the reported low-density bulk mat of SWCNT (0.7 W m^{-1} K^{-1}).[36] It is noted that the introduction of functional groups results in a lower thermal conductivity for SWCNT-OH (0.37 W m^{-1} K^{-1}), SWCNT-COOH (0.41 W m^{-1} K^{-1}), and SWCNT-NH_2 (0.24 W m^{-1} K^{-1}), values which are comparable to CNT-based composites.[15,35] This is probably attributed to two reasons, the residual polymer surfactant on the surface of the SWCNTs leading to interfacial barriers, and the introduction of functional groups inducing many defects in SWCNTs.[37] Although the TE power factor has a slight increase in SWCNT-OH, the enhanced ZT value of 3.8×10^{-2} has been achieved by the functional –OH due to the decreased thermal conductivity. Therefore, the introduction of functional groups in SWCNTs is valuable for guiding the rational optimization of TE performance for SWCNTs.

CONCLUSIONS

In summary, we have systematically investigated the TE performance of SWCNT films with different functional groups, such as hydroxyl, carboxyl, and amino. It can be found that the functionalization has resulted in the structure defects on SWCNTs and the conversion from metallic or semi-metallic of SWCNTs to semi-conductor leading to a lower electrical conductivity and higher Seebeck coefficient compared with pure SWCNT film. The SWCNT-OH achieves the maximum power factor of 47.8 μW m^{-1} K^{-2}. Simultaneously, the functionalization allows the significant reduction of in-plane thermal conductivity for SWCNT films. Eventually, the SWCNT-OH film gains an enhanced ZT of 3.8×10^{-2} which is twice as high as pure SWCNTs due to the large increase in Seebeck coefficient and reduction of thermal conductivity by the introduction of –OH in the sidewall of the SWCNTs. Therefore, the functionalization is an alternative strategy for regulating the TE properties of SWCNTs, and further in-depth studies will focus on the density of more different types and density of functional groups.

ACKNOWLEDGMENTS

This work was supported by the financial support of National Natural Science Foundation of China (51762018, 51572117, 11564015, and 51863009), the Innovation Driven “5511” Project of Jiangxi Province (20165BCB18016), and the Natural Science Foundation of Jiangxi Province (20181ACB20010).

REFERENCES

1. A.I. Hochbaum and P.D. Yang, *Chem. Rev.* 110, 527 (2010).
2. L.E. Bell, *Science* 321, 1457 (2008).
3. F.X. Jiang, J.K. Xu, B. Lu, and L.F. Li, *Chin. Phys. Lett.* 25, 2202 (2008).
4. B.Y. Lu, C.C. Liu, S. Lu, J.K. Xu, F.X. Jiang, Y.Z. Li, and Z. Zhang, *Chin. Phys. Lett.* 27, 057201 (2010).
5. F.F. Kong, C.C. Liu, J.K. Xu, F.X. Jiang, B.Y. Lu, R.R. Yue, G. Liu, and J. Wang, *Chin. Phys. Lett.* 28, 037201 (2011).
6. H. Shi, C.C. Liu, Q.L. Jiang, and J.K. Xu, *Adv. Electron. Mater.* 1, 1500017 (2015).
7. T.Z. Wang, C.C. Liu, X.D. Wang, X. Li, F.X. Jiang, C.C. Li, J. Hou, and J.K. Xu, *J. Polym. Sci. Part B: Polym. Phys.* 55, 997 (2017).
8. T.Z. Wang, C.C. Liu, J.K. Xu, Z.Y. Zhu, E.D. Liu, Y.J. Hu, C.C. Li, and F.X. Jiang, *Nanotechnology* 27, 285703 (2016).
9. C. Meng, C. Liu, and S. Fan, *Adv. Mater.* 22, 535 (2010).
10. C.A. Hewitt, A.B. Kaiser, S. Roth, M. Craps, R. Czerw, and D.L. Carroll, *Nano Lett.* 12, 1307 (2012).
11. W. Zhou, Q. Fan, Q. Zhang, L. Cai, K. Li, X. Gu, F. Yang, N. Zhang, Y. Wang, H. Liu, W. Zhou, and S. Xie, *Nat. Commun.* 8, 14886 (2017).
12. Q. Yao, L. Chen, W. Zhang, and X. Chen, *ACS Nano* 4, 2445 (2010).

13. C. Yu, K. Choi, and J.C. Grunlan, *ACS Nano* 5, 7885 (2011).
14. Q.L. Jiang, X.Q. Lan, C.C. Liu, H. Shi, Z.Y. Zhu, F. Zhao, J.K. Xu, and F.X. Jiang, *Mater. Chem. Front.* 2, 679 (2018).
15. J.L. Blackburn, A.J. Ferguson, C. Cho, and J.C. Grunlan, *Adv. Mater.* 30, 1704386 (2018).
16. G. Zhang and B. Li, *Nanoscale* 2, 1058 (2010).
17. Y. Nonoguchi, K. Ohashi, R. Kanazawa, K. Ashiba, K. Hata, T. Nakagawa, C. Adachi, T. Tanase, and T. Kawai, *Sci. Rep.* 3, 3344 (2013).
18. C.W. Padgett and D.W. Brenner, *Nano Lett.* 4, 1051 (2004).
19. C. Yu, A. Murali, K. Choi, and Y. Ryu, *Energy Environ. Sci.* 5, 9481 (2012).
20. J. Chen, H. Liu, D. Waldeck, and G. Walker, *J. Am. Chem. Soc.* 124, 9034 (2002).
21. J. Chen, M. Wang, B. Liu, K. Cui, and Y. Kuang, *J. Phys. Chem. B* 110, 11775 (2006).
22. E.P. Nguyen, B.J. Carey, J.Z. Ou, J.V. Embden, E.D. Gaspera, A.F. Chrimes, M.J. Spencer, S. Zhuiykov, K. Kalantarzadeh, and T. Daeneke, *Adv. Mater.* 27, 6225 (2015).
23. D. Voiry, A. Goswami, R. Kappera, C. Silva, D. Kaplan, T. Fujita, M. Chen, T. Asefa, and M. Chhowalla, *Nat. Chem.* 7, 45 (2015).
24. T.Z. Wang, C.C. Liu, F.X. Jiang, Z.F. Xu, X.D. Wang, X. Li, C.C. Li, J.K. Xu, and X.W. Yang, *Phys. Chem. Chem. Phys.* 19, 17560 (2017).
25. Y. Nakai, K. Honda, K. Yanagi, H. Kataura, T. Kato, T. Yamamoto, and Y. Maniwa, *Appl. Phys. Express* 7, 025103 (2014).
26. N.T. Hung, A.R. Nugraha, E.H. Hasdeo, M.S. Dresselhaus, and R. Saito, *Phys. Rev. B* 92, 165426 (2015).
27. A.A. Green and M.C. Hersam, *Nano Lett.* 8, 1417 (2008).
28. K.Z. Milowska and J.A. Majewski, *J. Chem. Phys.* 138, 194704 (2013).
29. J. Zhao, H. Park, J. Han, and J. Lu, *J. Phys. Chem. B* 108, 4227 (2004).
30. X.D. Wang, F. Meng, T.Z. Wang, C.C. Li, H. Tang, Z. Gao, S. Li, F.X. Jiang, and J.K. Xu, *J. Alloys Compd.* 734, 121 (2018).
31. D. Hayashi, Y. Nakai, H. Kyakuno, T. Yamamoto, Y. Miyata, K. Yanagi, and Y. Maniwa, *Appl. Phys. Express* 9, 125103 (2016).
32. Y. Nonoguchi, Y. Iihara, K. Ohashi, T. Murayama, and T. Kawai, *Chem. Asian J.* 11, 2423 (2016).
33. W. Zhou, J. Vavro, N.M. Nemes, J.E. Fischer, F. Borondics, K. Kamarás, and D.B. Tanner, *Phys. Rev. B* 71, 205423 (2005).
34. D. Hayashi, T. Ueda, Y. Nakai, H. Kyakuno, Y. Miyata, T. Yamamoto, T. Saito, K. Hata, and Y. Maniwa, *Appl. Phys. Express* 9, 025102 (2016).
35. X. Wang, H. Wang, and B. Liu, *Polymers* 10, 1196 (2018).
36. J. Hone, M. Whitney, and A. Zettl, *Synth. Met.* 103, 2498 (1999).
37. C. Yu, Y.S. Kim, D. Kim, and J.C. Grunlan, *Nano Lett.* 8, 4428 (2008).